

# LOCATION OPTIMIZATION FOR A GROUP OF TOWER CRANES

By P. Zhang,<sup>1</sup> F. C. Harris,<sup>2</sup> P. O. Olomolaiye,<sup>3</sup> and G. D. Holt<sup>4</sup>

**ABSTRACT:** A computerized model to optimize location of a group of tower cranes is presented. Location criteria are balanced workload, minimum likelihood of conflicts with each other, and high efficiency of operations. Three submodels are also presented. First, the initial location model classifies tasks into groups and identifies feasible location for each crane according to geometric "closeness." Second, the former task groups are adjusted to yield smooth workloads and minimal conflicts. Finally, a single-tower-crane optimization model is applied crane by crane to search for optimal location in terms of minimal hook transportation time. Experimental results and the steps necessary for implementation of the model are discussed.

## INTRODUCTION

On large construction projects several cranes generally undertake transportation tasks, particularly when a single crane cannot provide overall coverage of all demand and supply points, and/or when its capacity is exceeded by the needs of a tight construction schedule. Many factors influence tower crane location. In the interests of safety and efficient operation, cranes should be located as far apart as possible to avoid interference and collisions, on the condition that all planned tasks can be performed. However, this ideal situation is often difficult to achieve in practice; constrained work space and limitations of crane capacity make it inevitable that crane areas overlap. Subsequently, interference and collisions can occur even if crane jibs work at different levels. Crane position(s) tend to be determined through trial and error, based on site topography/shape and overall coverage of tasks. The alternatives for crane location can be complex, so managers remain confronted by multiple choices and little quantitative reference.

Crane location models have evolved over the past 20 years. Warszawski (1973) established a time-distance formula by which quantitative evaluation of location was possible. Furu-saka and Gray (1984) presented a dynamic programming model with the objective function being hire cost, but without consideration of location. Gray and Little (1985) optimized crane location in irregular-shaped buildings while Wijesundera and Harris (1986) designed a simulation model to reconstruct operation times and equipment cycles when handling concrete. Farrell and Hover (1989) developed a database with a graphical interface to assist in crane selection and location. Choi and Harris (1991) introduced another model to optimize single tower crane location by calculating total transportation times incurred. Emsley (1992) proposed several improvements to the Choi and Harris model. Apart from these algorithmic approaches, rule-based systems have also evolved to assist decisions on crane numbers and types as well as their site layout, e.g., CRANES (Gray and Little 1985); LOCRANE (Warszawski 1990).

The shortcomings of existing location models must be addressed to move them from the realms of research to regular

use by practitioners. First, existing models tend to oversimplify and site conditions are not considered. Further, little attempt has been made to model optimum location for a tower crane group. Therefore, it was first necessary to create a "more realistic" model for crane location in which these factors are considered; then, to develop the model for locating a group of tower cranes.

## Assumptions

Site managers were interviewed to identify their concerns and observe current approaches to the task at hand. Further, operations were observed on 14 sites where cranes were intensively used (four in China, six in England, and four in Scotland). Time studies were carried out on four sites for six weeks, two sites for two weeks each, and two for one week each. Findings suggested inter alia that full coverage of working area, balanced workload with no interference, and ground conditions are major considerations in determining group location. Therefore, efforts were concentrated on these factors (except ground conditions because site managers can specify feasible location areas). The following four assumptions were applied to model development (detailed later):

1. Geometric layout of all supply (S) and demand (D) points, together with the type and number of cranes, are predetermined.
2. For each S-D pair, demand levels for transportation are known, e.g., total number of lifts, number of lifts for each batch, maximum load, unloading delays, and so on.
3. The duration of construction is broadly similar over the working areas.
4. The material transported between an S-D pair is handled by one crane only.

## MODEL DESCRIPTION

Three steps are involved in determining optimal positions for a crane group. First, a location generation model produces an approximate task group for each crane. This is then adjusted by a task assignment model. Finally, an optimization model is applied to each tower in turn to find an exact crane location for each task group.

### Initial Location Generation Model

#### Lift Capacity and "Feasible" Area

Crane lift capacity is determined from a radius-load curve where the greater the load, the smaller the crane's operating radius. Assuming a load at supply point (S) with the weight  $w$ , its corresponding crane radius is  $r$ . A crane is therefore unable to lift a load unless it is located within a circle with radius  $r$  [Fig. 1(a)]. To deliver a load from (S) to demand point (D), the crane has to be positioned within an elliptical area

<sup>1</sup>Doctoral Candidate, School of Engrg. and Built Envir., Univ. of Wolverhampton, Wulfruna St., Wolverhampton WV1 1SB, U.K.

<sup>2</sup>Prof. of Constr. Sci., School of Engrg. and Built Envir., Univ. of Wolverhampton, Wolverhampton, U.K.

<sup>3</sup>Assoc. Dean, School of Engrg. and Built Envir., Univ. of Wolverhampton, Wolverhampton, U.K.

<sup>4</sup>Reader in Constr. Mgmt., School of Engrg. and Built Envir., Univ. of Wolverhampton, Wolverhampton, U.K. E-mail: G.D.Holt@wlv.ac.uk

Note. Discussion open until September 1, 1999. To extend the closing date one month, a written request must be filed with the ASCE Manager of Journals. The manuscript for this paper was submitted for review and possible publication on February 12, 1996. This paper is part of the *Journal of Construction Engineering and Management*, Vol. 125, No. 2, March/April, 1999. ©ASCE, ISSN 0733-9634/99/0002-0115-0122/\$8.00 + \$.50 per page. Paper No. 12203.

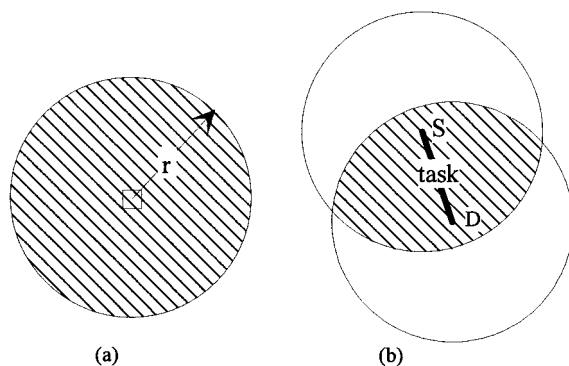


FIG. 1. Feasible Area of Crane Location for Task

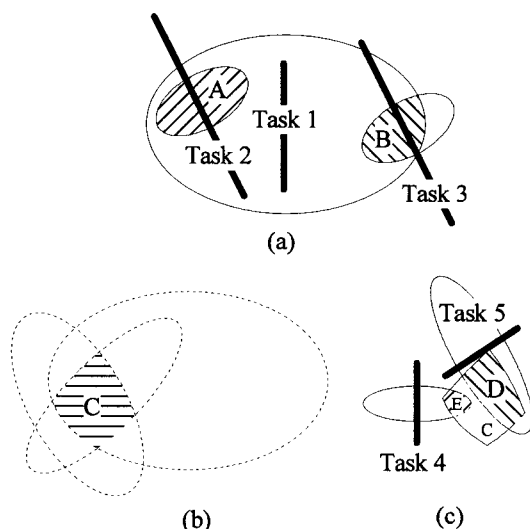


FIG. 2. Task "Closeness"

enclosed by two circles, shown in Fig. 1(b). This is called the feasible task area. The size of the area is related to the distance between *S* and *D*, the weight of the load, and crane capacity. The larger the feasible area, the more easily the task can be handled.

#### Measurement of "Closeness" of Tasks

Three geometric relationships exist for any two feasible task areas, as illustrated in Fig. 2; namely, (a) one fully enclosed by another (tasks 1 and 2); (b) two areas partly intersected (tasks 1 and 3); and (c) two areas separated (tasks 2 and 3). As indicated in cases (a) and (b), by being located in area *A*, a crane can handle both tasks 1 and 2, and similarly, within *B*, tasks 1 and 3. However, case (c) shows that tasks 2 and 3 are so far from each other that a single tower crane is unable to handle both without moving location; so more than one crane or greater lifting capacity is required. The closeness of tasks can be measured by the size of overlapping area, e.g., task 2 is closer to task 1 than task 3 because the overlapping area between tasks 1 and 2 is larger than that for 1 and 3. This concept can be extended to measure closeness of a task to a task group. For example, area *C* in Fig. 2(b) is a feasible area of a task group consisting of three tasks, where task 5 is said to be closer to the task group than task 4 since the overlapping area between *C* and *D* is larger than that between *C* and *E*. If task 5 is added to the group, the feasible area of the new group would be *D*, shown in Figure 2(c).

#### Grouping Tasks into Separated Classes

If no overlapping exists between feasible areas, two cranes are required to handle each task separately if no other

alternatives—such as cranes with greater lifting capacity or replanning of site layout—are allowed. Similarly, three cranes are required if there are three tasks in which any two have no overlapping areas. Generally, tasks whose feasible areas are isolated must be handled by separate cranes.

These *initial tasks* are assigned respectively to different (crane) task groups as the first member of the group, then all other tasks are clustered according to proximity to them. Obviously, tasks furthest apart are given priority as initial tasks. When multiple choices exist, computer running time can be reduced by selecting tasks with smaller feasible areas as initial tasks. The model provides assistance in this respect by displaying graphical layout of tasks and a list of the size of feasible area for each. After assigning an initial task to a group, the model searches for the closest remaining task by checking the size of overlapping area, then places it into the task group to produce a new feasible area corresponding to the recently generated task group. The process is repeated until there are no tasks remaining having an overlapping area within the present group. Thereafter, the model switches to search for the next group from the pool of all tasks, the process being continued until all task groups have been considered. If a task fails to be assigned to a group, a message is produced to report which tasks are left so the user can supply more cranes or, alternatively, change the task layout and run the model again.

#### Initial Crane Location

When task groups have been created, overlapping areas can be formed. Thus, the initial locations are automatically at the geometric centers of the common feasible areas, or anywhere specified by the user within common feasible areas.

#### Task Assignment Model

Group location is determined by geometric "closeness." However, one crane might be overburdened while others are idle. Furthermore, cranes can often interfere with each other so task assignment is applied to those tasks that can be reached by more than one crane to minimize these possibilities.

#### Accessibility Matrix

At this stage, it is assumed that all cranes are located at their respective initial locations. The accessibility matrix in Table 1 is then used to explicate the accessibility of each crane to its associated tasks, in which  $\delta_{ij}$  is a binary variable, defined as

$$\delta_{ij} = \begin{cases} 1 & \text{if crane } i \text{ is able to handle job } j \\ 0 & \text{otherwise} \end{cases}$$

Clearly, the task assignments are further required to apply for those reachable by more than one crane, i.e., for any  $j \in \bar{J} = \{j: \sum_i \delta_{ij} > 1\}$ .

#### Criteria of Task Assignment

Two criteria are applied to measure assignment effectiveness: balanced workloads in terms of respective transportation

TABLE 1. Accessibility Matrix

Cranes (1)	Tasks					
	Task <sub>1</sub> (2)	Task <sub>2</sub> (3)	... (4)	Task <sub>j</sub> (5)	... (6)	Task <sub>i</sub> (7)
Crane <sub>1</sub>	$\delta_{11}$	$\delta_{12}$				
Crane <sub>2</sub>	$\delta_{21}$	$\delta_{22}$				
...						
Crane <sub>i</sub>				$\delta_{ij}$		
...						
Crane <sub>i</sub>						$\delta_{ii}$

time for each crane, and lowest possibility of conflict. Balanced workload condition can be measured by the standard deviation of  $T_i$ , from

$$\sigma = \sqrt{\sum_i \frac{(\bar{T} - T_i)^2}{I}} = \sigma(\delta_{11}, \delta_{12}, \dots, \delta_{21}, \delta_{22}, \dots, \delta_{ij}, \dots, \delta_{II})$$

where  $T_i$  = transportation time of  $i$ th crane hook, and is given by

$$T_i = \sum_{j=1}^J \delta_{ij} \cdot Q_j \cdot (t_{ij}^1 + t_{ij}^2 + t_{ij}^3 + t_{ij}^4)$$

where  $(t_{ij}^1 + t_{ij}^2 + t_{ij}^3 + t_{ij}^4)$  = transportation time of  $i$ th crane performing  $j$ th tasks, and  $t_{ij}^1, t_{ij}^2, t_{ij}^3$ , and  $t_{ij}^4$  =, respectively, hook travel time with load, the one without load, the means of loading delay, and unloading delay;  $Q_j$  = number of lift of  $j$ th task; and  $\bar{T} = 1/I \cdot \sum_i T_i$ , the mean of transportation time of all cranes.

To measure possibility of conflict, a parameter (NC), called the *conflict index* is introduced. Each  $\delta_{ij}$  corresponds to a triangle with apexes representing the supply point, demand point, and crane location (Fig. 3). If two triangles are apart as in 3(a), no conflict happens. The number of intersections between two triangles reflects the severity of conflicts, i.e., the more intersections the more likely are conflicts. Hence, conflict in 3(c) is more probable than in 3(b). Additionally, the intensity of material flows also affects possibility of conflicts. Therefore, let  $n_{ij,kl}$  define the number of intersections of the two triangles, respectively, consisting of crane  $i$  and task  $j$ , crane  $k$  and task  $l$ . The possibility of conflicts between two crane-task pairs should be proportionate to  $n_{ij,kl}(Q_{ij} + Q_{kl})$ ,  $Q_{ij}$ , and  $Q_{kl}$ , being the number of lift of  $j$ th and  $l$ th tasks, respectively, in  $i$ th and  $k$ th task groups. Hence, conflicts between cranes  $i$  and  $k$  can be represented as

$$NC_{ik} = \sum_{l=1}^L \sum_{j=1}^J n_{ij,kl} (Q_{ij} + Q_{kl})$$

Obviously,  $n_{ij,kl}$  is closely related to  $\delta_{ij}$ , which depends on the

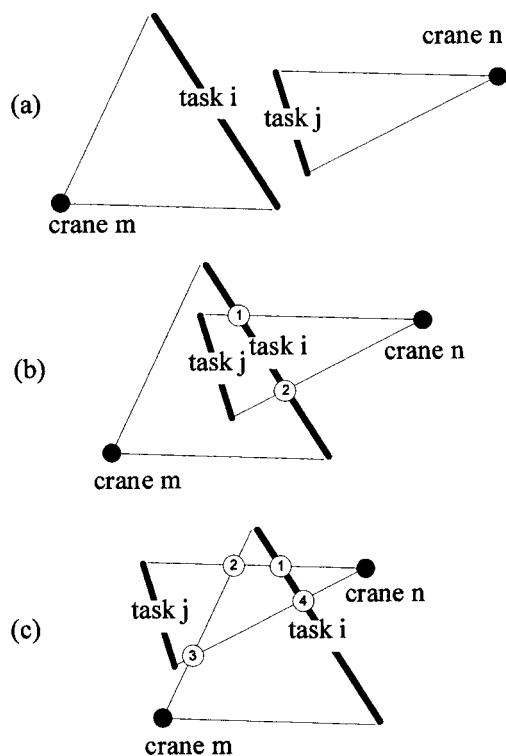


FIG. 3. Severity of Conflicts

results of task assignment. For all cranes and all tasks, the conflict index (reflecting general possibility of conflicts) can now be calculated as

$$NC = \sum_{i=1}^{I-1} \sum_{l=1}^I NC_{ik} = NC(\delta_{11}, \delta_{12}, \dots, \delta_{21}, \delta_{22}, \dots, \delta_{ij}, \dots, \delta_{II})$$

#### Task Assignment Algorithm

By integrating the above two criteria, task assignment can be represented as follows:

$$\min \left\{ NC(\bar{x}, \bar{y}, \delta_{11}, \delta_{12}, \dots, \delta_{21}, \delta_{22}, \dots, \delta_{ij}, \dots, \delta_{II}) \right\}$$

where the variables  $\delta_{ij}$  are those whose  $j \in \tilde{J} = \{j: \sum_i \delta_{ij} > 1\}$  and  $(\bar{x}, \bar{y})$  are locations of the cranes produced by the initial location generation model, and are treated as constants at this stage. This model is an abnormal 0-1 integer programming, and is impossible to solve by conventional algorithms. No common optimal solution exists generally for both NC and  $\sigma$ . However, a satisfactory solution can be obtained by a trade-off between the two criteria, i.e., for each solution, i.e., a set

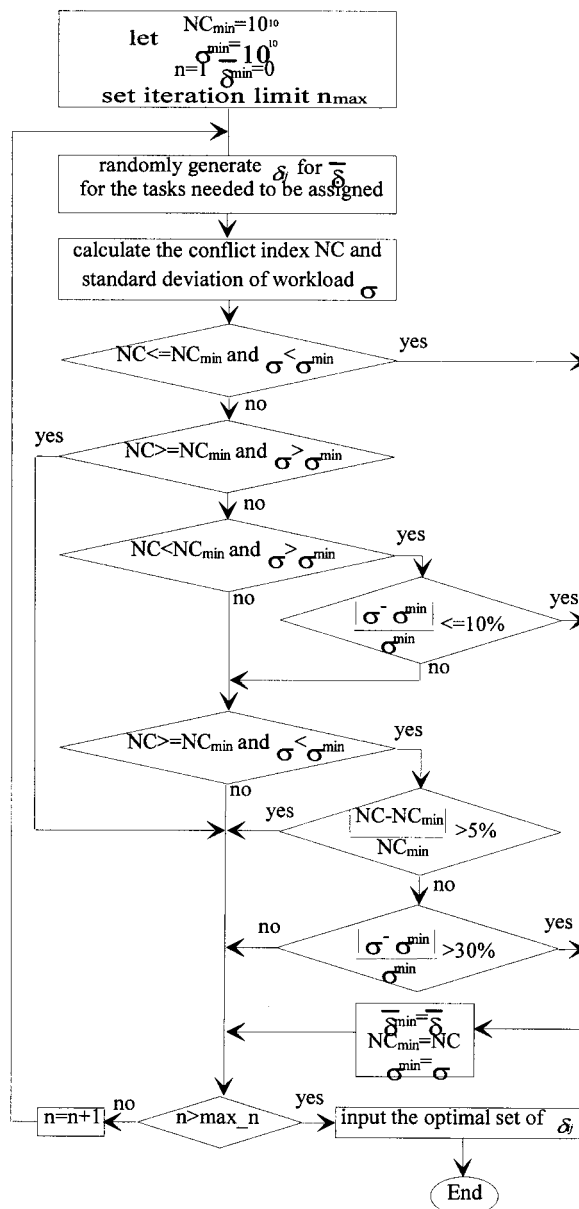


FIG. 4. Flow Chart of Task Assignment

of  $\delta_{ij}$  generally randomly, corresponding NC and  $\sigma$  are calculated. The best assignment solution is always replaced by the newly generated solution if the new solution can make (1) both NC and  $\sigma$  better; (2) NC better, but  $\sigma$  worse within acceptable scope (say 10%); and/or (3)  $\sigma$  better up to 30% but NC worse by no more than 5%. The purpose of this compromise is to accelerate iteration and put more emphasis on non-conflict consideration. The algorithm is represented as a flow chart in Fig. 4.

### Single Tower Crane Location Model

Every task is assigned uniquely to a group, together with balanced workloads and minimal possibilities of interference. However, each task group may correspond frequently with feasible areas rather than a single point; thus Monte-Carlo simulation is employed to determine the exact crane location, in terms of spatial layout and frequency of tasks, without changing the composition of the task groups. Let  $J$  denote the number of tasks in the  $i$ th crane task group, and  $Q_j$  the total number of repetitions of tasks  $j$  (lifts). Within  $Q_j$  there are  $K$  batches,  $N_j^k$  defined as the repeated number of task  $j$  in batch  $k$ , and  $P_j^k$  as the percentage of the tasks in batch  $k$  out of  $Q_j$ . A request represents a signal to indicate that the demand for a task  $j$  occurs, the average number of requests for task  $j$  being calculated by

$$R_j = \frac{Q_j}{\sum_{k=1}^K P_j^k \cdot N_j^k}$$

As an example,  $j$ th task is concrete handling with a total of 100 lifts ( $Q_j = 100$ ) between an S-D pair; the job is in batch manner, meaning that the deliveries are performed uninterrupted. The task consists of three batches ( $K = 3$ ), respectively, for different building-element pours: 70% total lifts (70 lifts) in 10-lift batch for slabs ( $N_j^1 = 10$ ,  $P_j^1 = 70\%$ ), 20% total lift (20 lifts) in 5-lift batch for columns, and finally 10% total lifts (10 lifts) in 2-lift batch for beams. Thus the average number of request times for task  $j$  is  $100/(0.7 \cdot 10 + 0.2 \cdot 5 + 0.1 \cdot 2) = 12$  (times). The frequency of requests for task  $j$  can be defined as

$$F_j = \frac{R_j}{\sum_{j=1}^J R_j}$$

By means of the above, a mechanism to simulate operation of the crane hook can be achieved by two random variables, the first representing occurrence of a request that could be any one of  $J$  possibilities, and the second the type of the batch within task  $j$ . For each realization of the random variable, its path is recorded and the hook transportation time spent on the  $m$ th request  $TR^{(m)}$  is calculated from

$$TR^{(m)} = T(D_j, S_j) + N_j^k \cdot [L(S_j) + T(S_j, D_j) + U(D_j) + T(D_j, S_j)] - T(D_j, S_j)$$

where  $T(D_j, S_j)$  = hook travel time without loads from  $D$  of task  $j'$  (produced by last request) to  $S$  of present request  $j$ ;  $T(S_j, D_j)$  = hook travel time with loads from  $S_j$  to  $D_j$ ;  $T(D_j, S_j)$  = hook travel time without loads from  $D_j$  to  $S_j$ ;  $L(S_j)$  = hook delay time for loading at  $S_j$ ; and  $U(D_j)$  = hook delay time for unloading at  $D_j$ . When the number of iterations  $M$  is large enough, average transportation time of hook (ATT) can be achieved by

$$ATT(x, y) = \frac{1}{M} \sum_{m=1}^M TR^{(m)}$$

Here,  $(x, y)$  are defined as discrete points in the feasible areas, and can be produced by gridding the feasible area. By applying simulation to all  $(x, y)$  one after another, a location with minimal average transportation time of hook ( $x^*, y^*$ ) is taken as optimal location, namely

$$ATT(x^*, y^*) = \min_{\text{for all } (x, y)} ATT(x, y)$$

The model mimics the whole process of delivery and produces a location where the crane is likely to complete tasks most quickly. Loading and unloading times are treated automatically as random variables with normal distributions; alternatively, the user is allowed to define a specific delay distribution.

### Hook Travel Time for Performing Task

If  $(XD_j, YD_j, ZD_j)$  and  $(XS_j, YS_j, ZS_j)$  refer, respectively, to the location of  $S$  and  $D$  of a task, for a crane located at  $(x, y)$ , hook travel time  $T$  can be expressed as  $T = \max(T_h, T_v) + \beta \cdot \min(T_h, T_v)$ . Here, hook vertical travel time  $T_v = V_v \cdot (Z_i - Z_j)$ ; hook horizontal travel time  $T_h = \max(T_a, T_\omega) + \alpha \cdot \min(T_a, T_\omega)$ ; and  $T_a, T_\omega$  = times for trolley radial and tangent movement, respectively, being calculated from (see Fig. 5)

$$\rho(D_j) = \sqrt{(XD_j - x)^2 + (YD_j - y)^2}$$

$$\rho(S_j) = \sqrt{(XS_j - x)^2 + (YS_j - y)^2}$$

$$l_j = \sqrt{(XD_j - XS_j)^2 + (YD_j - YS_j)^2}$$

Time for trolley radial movement:

$$T_a = \frac{|\rho(D_j) - \rho(S_j)|}{V_a}; T_\omega = \frac{1}{\omega} \cdot \text{Arc cos} \left( \frac{l_j^2 - \rho(D_j)^2 - \rho(S_j)^2}{2 \cdot \rho(D_j) \cdot \rho(S_j)} \right);$$

$$(0 \leq \text{Arc cos}(\theta) \leq \pi)$$

where  $V_a$  = radial velocity of trolley (m/min);  $\omega$  = slewing velocity of jib (r/min); and  $V_h$  = hoist velocity of hook (m/min). Here,  $\alpha$  and  $\beta$  are two parameters between 0 to 1;  $\alpha$  represents the degree of coordination of hook movement in radial and tangential directions in the horizontal plane; and  $\beta$  reflects those in the vertical and horizontal planes. There are two extreme situations for  $\alpha$ : simultaneous movement occurs when  $\alpha = 0$ , and consecutive movement when  $\alpha = 1$ , depending on the skill of the operator and the spaciousness of the site. For  $\beta$ , there are also two extreme situations: simultaneous

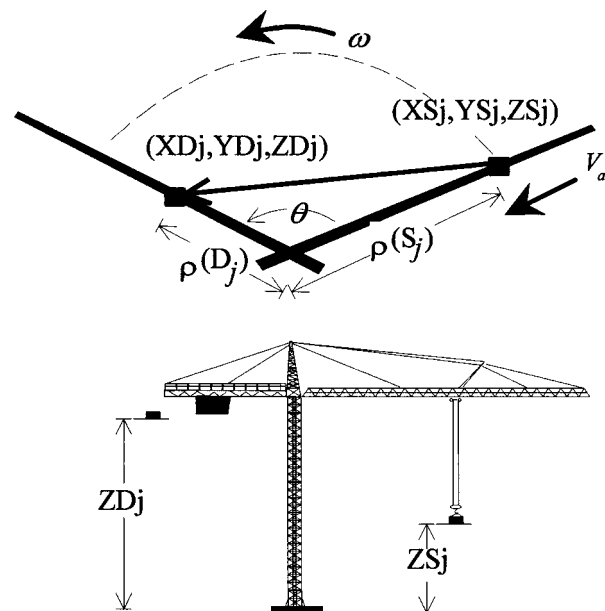


FIG. 5. Hook Travel Time

movement in two planes when  $\beta = 0$  or consecutive movement when  $\beta = 1$ . The value of  $\beta$  depends on the height of the working floor (the higher the floor, the greater is  $\beta$ ). Ideally, the value of both parameters need to be calibrated by observed data obtained from real construction sites. Kogan (1976) mentioned that an experienced driver performs simultaneous operations during 76% of the total duration of the cycle; thus, here the value of parameter  $\alpha$  is assumed as 0.25, unless otherwise stated, and  $\beta$  is assumed as 1, i.e., the hook moves consecutively in two planes.

### Location Optimization for Group of Tower Cranes

This can be realized by integrating the above three sub-models. If new NC and  $\sigma$  (corresponding with new crane locations) are improved, or at least NC declines while  $\sigma$  fluctuates within an acceptable range, the previous will be replaced by new ones and stored in the buffer. Otherwise, if new NC and  $\sigma$  deteriorate, the old remains, the task assignment model can then be resumed from the new crane location. When the cycles have been carried out sufficiently or the descent is no longer significant to make NC and  $\sigma$  better, crane locations in the buffer are considered optimal.

### MODEL EXPERIMENT

To investigate model effectiveness a hypothetical case was tested. The building is a reinforced concrete frame (Fig. 6) with a working floor at about 35 m height, and an elevator well. The main transportation tasks include deliveries of in situ concrete materials from seven supply points. The three hatched areas are feasible location areas permitted by site conditions, the building being simplified with 24 demand points. Data on the tasks, three cranes, and site boundaries are detailed in Appendix I.

### Model Output

Six sets of initial task-crane pairs were tested; outcomes for the first three sets {1(crane)-8(task), 2-25, 3-55}, {1-1, 2-26, 3-39}, and {1-24, 2-30, 3-71} are shown in Table 2, with primary task groups and corresponding feasible areas led by the initial location generation model illustrated in Fig. 7. The

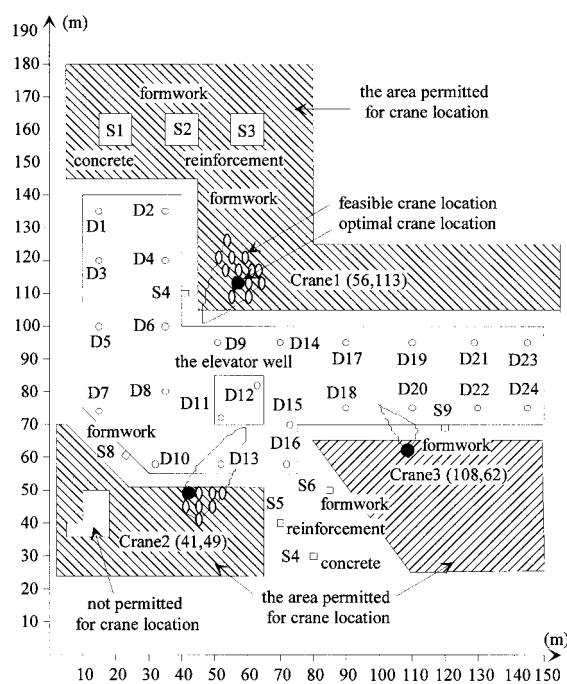


FIG. 6. Site Plan

TABLE 2. Major Output from First Three Sets of Input

Input	Test item	Set 1			Set 2			Set 3		
	Crane No.	1	2	3	1	2	3	1	2	3
Output	Initial Task No.	8	25	55	1	26	39	24	30	71
Initial task model output	NC	18496			18496			18496		
	$\sigma$ (min)	1584			1584			1584		
	Feasible area(M <sup>2</sup> )	593			280			139		
	Feasible area centre	(59,121)			(49,49)			(108,62)		
Assignment model output	NC	13053			13053			13053		
	$\sigma$	1292			1292			1292		
	Area (M <sup>2</sup> )	277			280			79		
Output of single tower crane location optimisation model	NC	13053			13053			13053		
	$\sigma$ (min)	1233			1233			1233		
	Optimal location	(56,113)			(41,49)			(108,62)		
	ATT	43.2			27.1			58.8		
	Workload (min)	7174			10082			9330		
	Workload rates	27%			38%			35%		

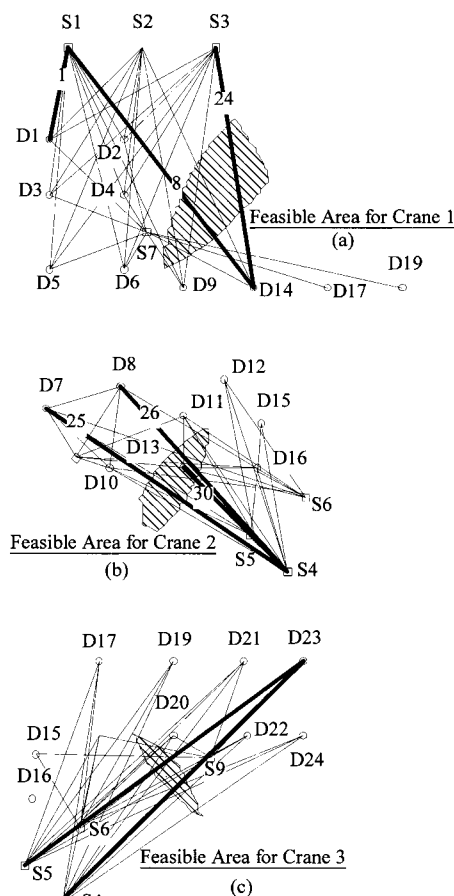


FIG. 7. Task Group and Feasible Areas by Generation Model

model started with three different sets of combinations of task and crane, but final task groups and resultant feasible areas were all identical. Subsequently, the center of the respective feasible areas was automatically passed to the task assignment model. After 2,000 iterations, the task assignment model produced a new task assignment with the conflict index 13,053 reduced from 18,496 and standard deviation of workload 1,292

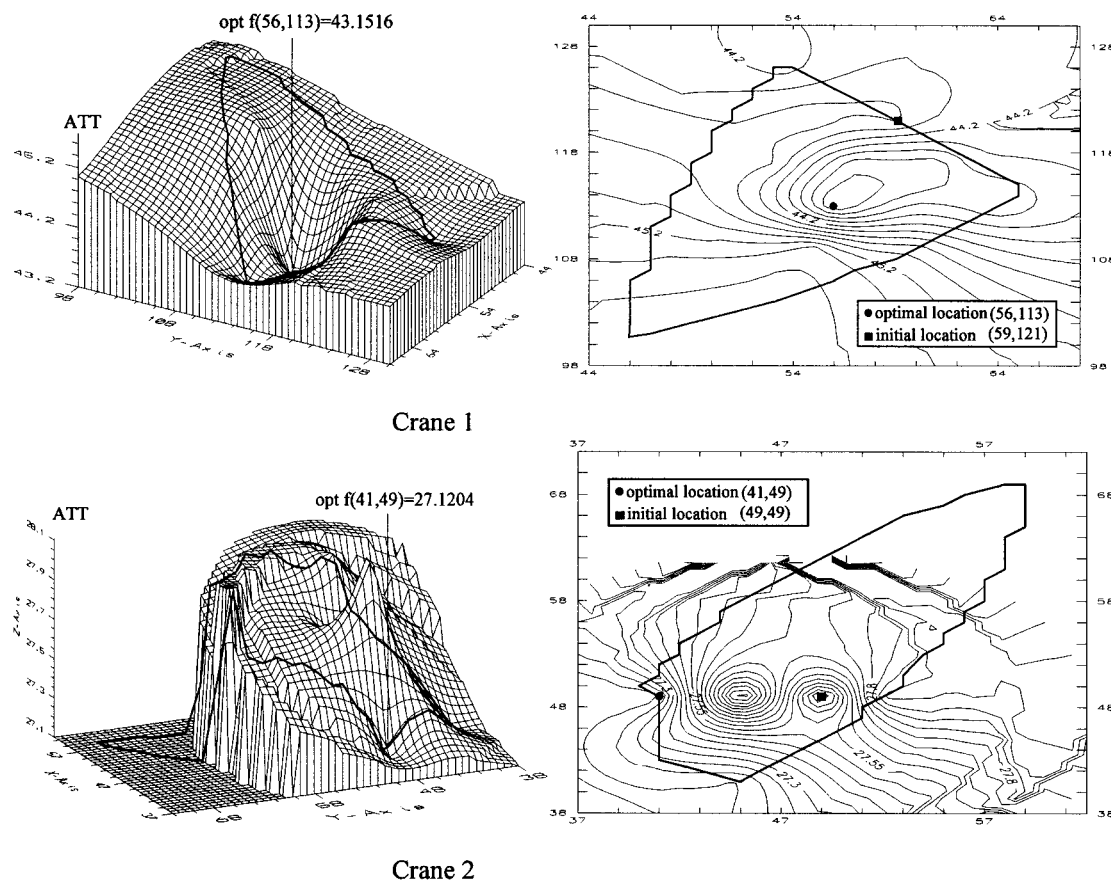


FIG. 8. Distribution of ATT for Cranes 1 and 2

TABLE 3. Major Output from Last Three Sets of Input

input	Test item	set 4			set 5			set 6		
	Crane No.	1	2	3	1	2	3	1	2	3
output	Task No.	55	25	8	55	8	25	25	8	55
initial task model	NC	306283			326908			159964		
	$\sigma$ (min)	4564			1422			5585		
	area(M <sup>2</sup> )	442	292	409	442	108	222	1131	108	140
output	Initial location	(97,85)	(46,54)	(44,127)	(97,85)	(44,128)	(56,68)	(75,82)	(44,128)	(109,65)
optimal solution after four round	NC	18183			37961			27331		
	$\sigma$ (min)	1809			1926			4340		
	Optimal location	(102,85)	(51,54)	(52,122)	(102,85)	(48,128)	(64,73)	(78,90)	(48,128)	(109,61)
circulation	area (M <sup>2</sup> )	442	129	52	442	108	50	364	108	140
	ATT	62.1	25.4	47.6	66.9	50.8	25.4	31.0	50.8	67.7
	Workload (min)	10735	9761	6503	9578	6322	10907	15070	6324	5461
	workload rate	40%	36%	24%	35%	24%	41%	56%	24%	20%

(min) reduced from 1,584, i.e., ameliorated respectively at approximately 30% and 20%. The corresponding feasible areas were also changed respectively, as shown in Fig. 6.

Discrete coordinates resulting from gridding the feasible areas are further checked, only those satisfying the requirements of the site conditions eventually forming final feasible locations. The single-tower-crane location model is thereafter applied to these points to start simulation, and finally produces average transportation time of hook at the points. Fig. 8 shows the distribution of ATT for cranes 1 and 2—but without crane 3, since there is only one feasible location for crane 3, as illustrated in Fig. 6. Optimal crane location is the one where the minimal ATT is achieved. However, once the crane is moved from its initial to its optimal location, the conflict index and standard deviation of workloads might be changed (but are assumed to remain unaltered in the course of location op-

timization), and should be calculated again. In this case, the conflict index for the new location remains the same while  $\sigma$  declines from 1,292 to 1,233, i.e., the best optimal locations so far are kept. The next round of task assignment can start from the present optimal locations. In this example, another three rounds are run. However, no improvement was achieved so the location produced for the first round is considered to be optimal (Fig. 6).

To explore how the model responded to various combinations of task-crane pairs in a larger range, another three sets of crane-task pairs were examined. For this purpose, the cranes were located inside the building; input and output are shown in Table 3. After four simulation rounds for each set of initial input, all conflict indexes and standard deviations of sets 4 and 5 reduced substantially. Apart from the data output, the user can also take advantage of the model's graphic display for

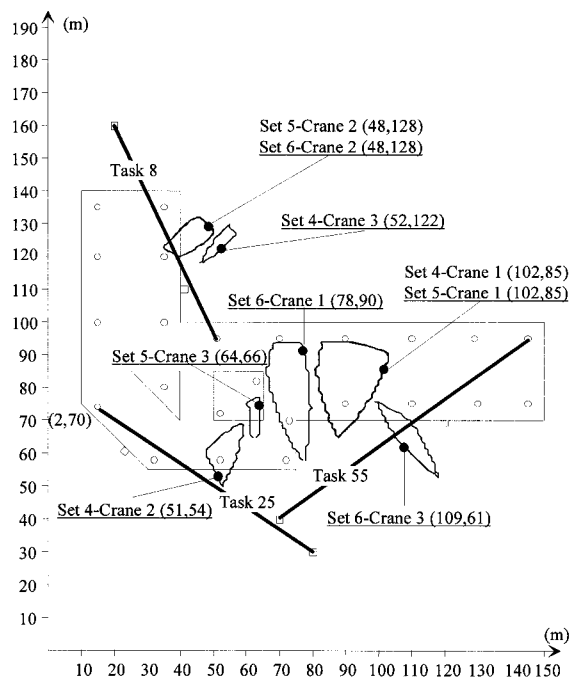


FIG. 9. Feasible Areas from Last Three Sets of Input

shape and size of feasible areas, illustrated in Fig. 9. In this case study, from the data and graphic output, the user may become aware that optimal locations led by test sets 1, 2, and 3 (Fig. 3) are the best choices (balanced workload, conflict possibility, and efficient operation). Alternatively, in connection with site conditions such as availability of space for the crane position and ground conditions for the foundation, site boundaries were restricted. Consequently, one of the cranes had to be positioned in the building. In this respect, the outcomes resulting from set 4 would be a good choice in terms of a reasonable conflict index and standard deviation of workload, provided that a climbing crane is available and the building structure is capable of supporting this kind of crane. Otherwise, set 5 results would be preferable with the stationary tower crane located in the elevator well, but at the cost of suffering the high possibility of interference and unbalanced workloads.

## CONCLUSIONS

Overall coverage of tasks tends to be the major criterion in planning crane group location. However, this requirement may not determine optimal location. The model helps improve conventional location methods, based on the concept that the workload for each crane should be balanced, likelihood of interference minimized, and efficient operation achieved. To do this, three submodels were highlighted. First, by classifying all tasks into different task groups according to geometric "closeness" an overall layout is produced. Second, based on a set of points located respectively in the feasible areas (initial location), the task assignment readjusts the groups to produce new optimal task groups with smoothed workloads and least possibility of conflicts, together with feasible areas created. Finally, optimization is applied for each crane one by one to find an exact location in terms of hook transport time in three dimensions.

Experimental results indicate that the model performs satisfactorily. In addition to the improvement on safety and average efficiency of all cranes, 10–40% savings of total hooks transportation time can be achieved. Effort has been made to model the key criteria for locating a group of tower cranes, and two real site data have been used to test the model. However, it does not capture all the expertise and experience of

site managers; other factors relating to building structure, foundation conditions, laydown spaces for materials, accessibility of adjoining properties and so on, also contribute to the problem of locations. Therefore, the final decision should be made in connection with these factors.

## APPENDIX I. DATA REQUIREMENTS

### Task Data

S1 and S4 are concrete loading points, S3 and S5 the reinforcement workshop, S2 and S6 the formwork yards, and S7, S8, and S9 the loading platforms for previously used formwork waiting to be lifted to the working floor (Fig. 6). The number of lifts between S-D pairs is listed in Table A-1. The number between D-D pairs are for sundries lift.

Table A-2 lists the parameters related to a probabilistic distribution of loading and unloading delays, each task being allowed to have its own delay type and distribution parameter specified by the user. Similarly, the number of batches, size of batch, and maximum weight of lift are also assumed to be solely related to the type of materials handled (Table A-3).

### Crane Data

This consists of crane type technical parameters such as the load-radius profile, speeds of hook hoisting, trolley sliding, and boom slewing.

### Site Boundary Data

These are defined by the coordinates of polygons represented as allowed areas for locating cranes (Fig. 6).

TABLE A-1. Task Spatial and Frequency Distribution

	S1	S2	S3	S4	S5	S6	S7	S8	S9	D7	D8	D10	D11	D13	D15
D1	92	9	6				3								
D2	80	7	4				5								
D3	70	6	5				3								
D4	65	6	4				3								
D5	65	6	4				4								
D6	70	8	5				4								
D7				110	12	6		6				16			
D8				153	14	7		8		23					
D9	90	9	7				5								
D10				180	15	9		7			14				
D11				154	14	7		7							
D12				145	13	8	7								
D13				110	12	6		4					9		
D14	90	9	7				5								
D15				94	110	6			5						
D16				120	11	8		6						21	16
D17				88	7	4	3								
D18				91	8	5			5						
D19				79	6	6	3								
D20				83	9	4			4						
D21				84	9	5			3						
D22				78	7	6			6						
D23				99	10	6			5						
D24				104	11	7			7						

TABLE A-2. Statistic Parameters for Delay

Material (1)	Load Delay (minimum)		Unload Delay (minimum)	
	Mean $\mu$ (2)	Standard deviation $\sigma$ (3)	Mean $\mu$ (4)	Standard deviation $\sigma$ (5)
Concrete	3	1	4	2
Formwork	2	0.5	2	0.7
Reinforcement	2	0.5	2	0.7
Sundries	2	1	4	2

TABLE A-3. Size of Lift Batches

Material (1)	Maximum weight of lift (7) (2)	Batch 1		Batch 2		Batch 3	
		Number of lifts (3)	Percent (%) (4)	Number of lifts (5)	Percent (%) (6)	Number of lifts (7)	Percent (%) (8)
Concrete	1	30	80	4	15	2	5
Formwork	1.2	2	100	—	—	—	—
Reinforcement	1.3	1	100	—	—	—	—
Sundries	1.2	1	100	—	—	—	—

## APPENDIX II. BIBLIOGRAPHY

- Alhussein, M., Alkass, S., and Moselhi, O. (1995). "A computer integrated system for crane selection." *Proc., 6th Int. Conf. on Civ. and Struct. Engrg. Computing*, Volume: Development in computer aided design and modelling for civil engineering, CIVIL-COMP Press, Edinburgh, U.K., 43–48.
- Alkass, A., Aronian, A., and Moselhi, O. (1994). "Computer-aided equipment selection for transporting and placing concrete." *J. Constr. Engrg. and Mgmt.*, ASCE, 119(3), 445–465.
- Borland C++ manuals. (1993). Borland International, Inc., Scotts Valley, Calif.
- Dickie, D. E., and Short, D. (1981). *Crane handbook*, revised U.K. ed. Butterworth, London.
- Harris, F. C. (1991). *Modern construction equipment and methods*. Longman Science and Technology, London, U.K.
- Harris, F. C., and McCaffer, R. (1991). "Management of contractors plant." *Technical Information Service*, Chartered Inst. of Building, U.K., No. 127.
- Herbert, P. F. (1974). "Vertical movement of materials on high rise building." *Build. Technol. and Mgmt.*, 12(4).
- Illingworth, J. R. (1993). *Construction Methods and Planning*, 1st Ed., E & FN Spon, London.
- Rodriguez-Ramos, W. E., and Francis, R. L. (1983). "Single crane location optimisation." *J. Constr. and Mgmt.*, ASCE, 109(4), 387–396.
- Warszawski, A. (1985). "Decision model and expert system in construction management." *Build. and Envir.*, 20(4), 201–210.
- Wijesundera, D. A., and Harris, F. C. (1989). "The selection of materials handling methods in construction by simulation." *Constr. Mgmt. and Economics*, 7, 95–102.
- Wijesundera, D. A., Olomolaiye, P. O., and Harris, F. C. (1991). "Dynamic simulation applied to materials handling in high-rise construction." *Comp. and Struct.*, 41(6), 1133–1139.
- Zhang, P., Harris, F. C., Olomolaiye, P. O., and Goodwin, M. (1995). "A simulation model for optimising the location of a single tower crane."

*Proc., 6th Int. Conf. on Civ. and Struct. Engrg. Computing*, Vol: Development in computational techniques for civil engineering, CIVIL-COMP Press, Edinburgh, U.K., 25–32.

- Zhang, P., Harris, F. C., and Olomolaiye, P. O. (1996). "A computer-based model for optimising the location of a single tower crane." *Build. Res. and Inf.*, 24(2), 113–123.

## APPENDIX III. REFERENCES

- Choi, C. W., and Harris, F. C. (1991). "A model for determining optimum crane position." *Proc., Instn. Civ. Engrs.*, Institution of Civil Engineers, London, Part 1, 90, 627–634.
- Emsley, M. W. (1992). "Discussion on a model for the selection of the optimum crane for construction sites." *Proc., Instn. Civ. Engrs., Struct. and Buildings*, 94, 503–504.
- Farrell, C. W., and Hover, K. C. (1989). "Computerised crane selection and placement for the construction site." *Proc., 4th Int. Conf. on Civ. and Struct. Engrg. Computing*, CIVIL-COMP Press, Edinburgh, U.K., 1.
- Furusaka, S., and Gray, C. (1984). "A model for the selection of the optimum crane for construction sites." *Constr. Mgmt. and Economics*, 2, 157–176.
- Gray, C., and Little, J. (1985). "A systematic approach to the selection of an appropriate crane for a construction site." *Constr. Mgmt. and Economics*, 3, 121–144.
- Kogan, J. (1976). *Crane design—Theory and calculation of reliability*. Wiley, New York.
- Warszawski, A. (1973). "Analysis of transportation methods in construction." *J. Constr. Div.*, ASCE, 99(1), 191–202.
- Warszawski, A. (1990). "Expert system for crane selection." *Constr. Mgmt. and Economics*, 8, 179–190.
- Wijesundera, D. A., and Harris, F. C. (1986). "Computer simulation for materials handling in high rise construction." *Proc., Int. AMSE Conf. on Modelling and Simulation*, Sorrento, Italy, 4.4, 81–95.